STEM CELLS®
TECHNOLOGY DEVELOPMENT

Metabolic Changes in Mesenchymal Stem Cells in Osteogenic Medium Measured by Autofluorescence Spectroscopy

JOHANN M.G. REYES,[a] SARA FERMANIAN,[b] FAN YANG,[b] SHI-YOU ZHOU,[a] SAMANTHA HERRETES,[a] DOUGLAS B. MURPHY,[c] JENNIFER H. ELISSEEFF,[b] ROY S. CHUCK[a]

Departments of [a]Ophthalmology, [b]Biomedical Engineering, and [c]Cell Biology, Johns Hopkins University, Baltimore, Maryland, USA

Key Words. Bone marrow • Mesenchymal stem cells • Fluorescence microscopy • Differentiation

ABSTRACT

The purpose of this study was to measure metabolic changes in mesenchymal stem cells (MSCs) placed in osteogenic medium by autofluorescence spectroscopy. MSCs were plated in stem cell-supporting or osteogenic medium and imaged. Shift from the basic growth environment to the inductive osteogenic environment was confirmed by reverse transcription-polymerase chain reaction. Reduced pyridine nucleotides were detected by exciting near 366 nm and measuring fluorescence at 450 nm, and oxidized flavoproteins were detected by exciting at 460 nm and measuring fluorescence at 540 nm. The ratio of these fluorescence measurements, reduction-oxidation (redox) fluorometry, is a noninvasive measure of the cellular metabolic state. The detected pyridine nucleotide to flavoprotein ratio decreased upon transitioning from the stem cell to the differentiated state, as well as with increasing cell density and cell-cell contact. MSC metabolism increased upon placement in differentiating medium and with increasing cell density and contact. Redox fluorometry is a feasible, noninvasive technique for distinguishing MSCs from further differentiated cells. STEM CELLS *2006;24:1213–1217*

INTRODUCTION

Adult bone marrow-derived mesenchymal stem cells have been demonstrated to be pluripotent for differentiation into such tissues as bone, cartilage, and tendon [1–3]. Standard techniques now exist to culture these stem cells in vitro for experimental study and manipulation. It has been shown that differentiation along different pathways may be controlled by medium as well as substrate [4, 5]. Although much effort has been expended in searching for stem cell probes, currently there still exists no reliably specific marker for stem cells of any type [6]. In addition, many of the markers that have been proposed and studied are invasive to the cell or cell surface and may alter or even kill the cell.

One of the most accepted properties of stem cells is their ability to slowly cycle and continuously replenish cell populations [7]. We hypothesize that such slowly cycling cells may be characterized by slower intrinsic metabolism. If so, then these slowly cycling populations should be detectable by the noninvasive metabolic autofluorescence spectroscopic technique of reduction-oxidation (redox) fluorometry.

Redox Fluorometry

Redox fluorometry is an optical spectroscopic method for estimating the amount of reduced pyridine nucleotides and oxidized flavoproteins in living tissue. Fluorescence emission detected in the region of 450 nm after excitation at 366 nm contains components from reduced pyridine nucleotides (NADH and NADPH) in the cytoplasm and mitochondria, with greater quantum yield from the mitochondrial-bound species. Fluorescence detected in the region of 540 nm after excitation at 460 nm measures the cellular levels of the flavoproteins lipoamide dehydrogenase and electron transfer flavoprotein, which exist mostly as cofactors for enzymes involved in redox reactions. The ratio of these fluorescence measurements, which minimizes interfering factors such as absorption of excitation and emission light by other intrinsic chromophores, light scattering, and variations in mitochondrial density and flavoprotein concentration, has previously been proposed as a noninvasive measure of the organ cellular metabolic state [8–10]. More recently, the development of two-photon femtosecond laser excitation and scanning confocal microscopy allows three-dimensional mapping of cellular metabolic oxidation/reduction states in situ with high resolution [11–13].

Redox fluorometry has also been applied to the detection of cells with deregulated proliferative potential. Using this noninvasive spectroscopic technique, normal and transformed fibroblasts

Correspondence: Roy S. Chuck, M.D., Ph.D., Wilmer Ophthalmological Institute, Johns Hopkins University, 3-127 Jefferson Building, 600 North Wolfe St., Baltimore, Maryland 21117, USA. Telephone: 410-502-1923; Fax: 443-287-1514; e-mail: rchuck1@jhmi.edu Received November 22, 2004; accepted for publication December 14, 2005; first published online in STEM CELLS *EXPRESS* January 26, 2006. 1066-5099/2006/$20.00/0 doi: 10.1634/stemcells.2004-0324

have been separated [14], as have proliferating and nonproliferating epithelial cells [15]. More recently, others have discovered that the intracellular redox state appears to be a necessary and sufficient modulator of the balance between self-renewal and differentiation in dividing optic nerve oligodendrocyte type 2 astrocyte progenitor cells [16]. That is, the intracellular redox state of freshly isolated progenitors allows prospective isolation of cells with different self-renewal characteristics.

As described above, the noninvasive microscopic technique of redox fluorometry, which is based upon stimulated autofluorescence detection, has historically been suggested as a viable clinical measure of the cellular metabolic state. More recently, redox fluorometry has also been demonstrated to be able to differentiate between self-renewing and differentiating cells. Therefore, this simple technique may be useful in separating stem cells from further differentiated stages of development. Here, we demonstrate that mesenchymal stem cells may be isolated from further differentiated osteocytes by redox fluorometry in a tissue culture model.

MATERIALS AND METHODS

Mesenchymal Stem Cell Culture in Stem Cell and Osteogenic Medium

The following were used in mesenchymal stem cell growth medium (MSCGM) (Cambrex, Walkersville, MD, http://www.cambrex.com) [17]: 2 ml of MSCBM basal medium supplemented with two vials of 25 ml of fetal bovine serum (FBS) to attain an overall concentration of 10%, 10 ml of 200 mM L-glutamine, and 25 U of penicillin plus 25μg (0.5 ml) of streptomycin (MSCGM SingleQuots Bullet Kit; Cambrex). Subcultures were performed after treatment with Trypsin/EDTA 0.25 mg/m1 and trypsin neutralizing solution (TNS).

Osteogenic medium [18] consisted of Dulbecco's modified Eagle's medium (DMEM) without sodium pyruvate (Invitrogen, Carlsbad, CA, http://www.invitrogen.com), 100 nM dexamethasone (Sigma-Aldrich, St. Louis, http://www.sigmaaldrich.com), 50 M ascorbic acid-2-phosphate (Sigma-Aldrich), 10 mM glycerophosphate (Sigma-Aldrich), 10% FBS, 100 U/ml penicillin (Invitrogen), and 100 g/ml streptomycin (Invitrogen).

Mesenchymal Stem Cell Harvest and Isolation

Goat bone marrow-derived mesenchymal stem cells (MSCs) were prepared with guidance from and according to the method of Murphy et al. [19]. These cells obtained from bone marrow aspirates of adult goats are known to be homogeneously $SH4^+$/$CD14^-$ and $CD44^+$/$CD34^-$ [19]. The CD44 [20] and SH-4 [21] antibodies are known to label mesenchymal cells and not react with hematopoietic cells or with osteocytes. In contrast, MSCs are known to be negative for CD14 and CD34, lipopolysaccharide receptor markers of the hematopoietic lineage.

Bone marrow samples from goat femurs (Thomas Morris, Inc., Reisterstown, MD) were washed and centrifuged (1,000 rpm for 10 minutes) twice in medium (Cambrex) and resuspended in fresh medium thereafter. Mononuclear cells were counted using a hemocytometer and were plated in culture flasks at a density of 120,000 cells/cm^2. The culture medium was changed after 4 days and then every 2–3 days thereafter until confluence.

Freezing and Thawing Cells

Cells were centrifuged, and the medium was aspirated and replaced with an appropriate amount of freezing medium: 40% MSCGM, 50% FBS, and 10% dimethyl sulfoxide. The cells were then aliquoted into cryo-vials and frozen at a controlled rate of -1°C/minute at -80°C at a concentration of 2–3 million cells/ml. After 24 hours, the vials were transferred to liquid nitrogen for long-term storage. To thaw cells, the frozen vial was placed and gently swirled in a 37°C water bath.

Plating and Passaging Cells

After thawing, the concentrated cell solution (1–3 million cells/ml) was diluted with more medium to obtain a density of 5,000 cells/cm^2 for plating. Medium change was performed every 2–3 days. Upon reaching confluence (at approximately 5 days), the medium was aspirated, and the cells were rinsed with phosphate-buffered saline (PBS) to prepare them for passaging. After rinsing, the PBS was aspirated, and the cells were trypsinized for 5 minutes. Cell release from the culture plate was confirmed under microscopic visualization, and TNS was added to the solution to neutralize the trypsin. The solution was then placed in a centrifuge tube and spun for 10 minutes at 1,000 rpm. Trypsin was aspirated, and the cells were resuspended in fresh medium. The cells were counted and then were either replated for future passages or used for fluorescence imaging.

RNA Extraction and Reverse Transcription-Polymerase Chain Reaction

Goat MSCs were seeded at an initial density of 5,000 cells/cm^2 and cultured separately in MSCGM and osteogenic medium. After 1 week, total RNA was isolated from monolayer culture using the RNeasy minikit following the manufacturer's protocol (Qiagen, Valencia, CA, http://www1.qiagen.com). cDNA was synthesized by reverse transcription with the Superscript First-Strand Synthesis System (Invitrogen). Polymerase chain reaction (PCR) was performed using Taq DNA Polymerase (Invitrogen) at annealing temperature of 59°C (for β-actin and cbfa-1) for 35 cycles. The sequences of PCR primers (forward and backward, 5′ to 3′) were as follows: β-actin, 5′-TGGCACCACACCTTCTACAATGAGC-3′ and 5′-GCACAGCTTCTCCTTAATGTCACGC-3′; cbfa-1, 5′-CCACCCGGCCGAACTGGTCC-3′ and 5′-CCTCGTCCGCTCCGGCCCACA-3′. Each PCR product was analyzed by separating 4 μl of the amplicon and 1 μl of loading buffer in 2% agarose gel in Tris-acetic acid-EDTA buffer.

Autofluorescence Microscopy

All images were obtained using a Zeiss inverted microscope (Axiovert 200M; Carl Zeiss, Jena, Germany, http://www.zeiss.com) with a $\times$100 objective (FLUAR $\times$100, 1.3 oil). The microscope was equipped with a mercury lamp (HB 103) and a cooled charge-coupled device camera (Axiocam MRc5) for taking images. To detect intrinsic reduced pyridine nucleotides, a Carl Zeiss 4,6-diamidino-2-phenylindole filter set (excitation, G365; emission, bandpass 445/50) was used. Oxidized flavoproteins were identified using a Carl Zeiss fluorescein isothiocyanate filter set (excitation: bandpass 450–490, emission bandpass 515–565). To minimize photobleaching and light stimulation, the illumination source was turned off during fluorescence imaging. All the images and fluorescence ratios were processed and analyzed using AxioVision software (Carl Zeiss). Prior to autofluorescence microscopy, all cells were plated and expanded on glass

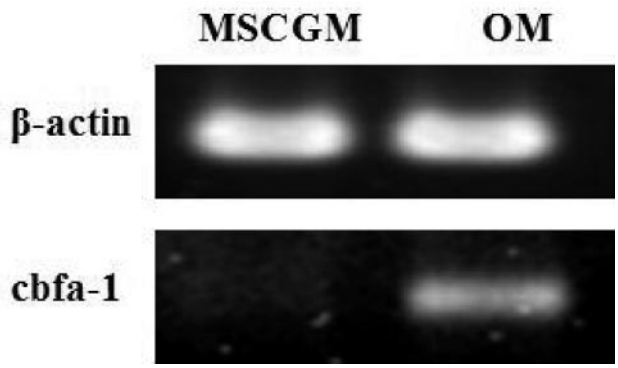

Figure 1. Reverse transcription-polymerase chain reaction of β-actin and cbfa-1 expression in MSCGM and OM. Abbreviations: MSCGM, mesenchymal stem cell growth medium; OM, osteogenic medium.

surfaces (Cultureware dishes; MatTek, Ashland, MA, http://mattek.com). In addition, cell cultures were equilibrated in colorless PBS solution before imaging.

Fluorescent Dyes and Subcellular Markers

To confirm the identity of autofluorescent cellular structures, labeling dyes were used to stain the specimens. MitoTracker Green FM and LysoTracker Red (Molecular Probes Inc., Eugene, OR, http://probes.invitrogen.com) were allowed to warm in room temperature and subsequently diluted with DMEM to the desired concentrations (30 and 75 nM, respectively). Cell culture medium was removed and replaced with the appropriate, prewarmed (37°C) probe-containing medium. Incubation was carried out for 30 minutes with MitoTracker Green FM and for 1 hour for LysoTracker Red. The cells were then washed with buffer solution and imaged with the appropriate Carl Zeiss FITC (excitation, bandpass 450–490; emission, bandpass 515–565) and rhodamine (excitation, bandpass 546/12; emission, bandpass 515–565) filter sets.

Results

Reverse transcription-PCR demonstrates that the early osteogenesis marker, transcriptional factor cbfa-1, was not expressed in MSCGM culture but was positively expressed in the monolayer cells in osteogenic culture, indicating that these cells differentiate down the osteogenic pathway once they are shifted from the basic growth environment to the inductive osteogenic environment (Fig. 1). In previous work, we have demonstrated that the osteogenic differentiation markers alkaline phosphatase and osteocalcin are expressed in these differentiated goat MSCs and that cbfa-1 expression is found in conjunction with production of these proteins [22]. The housekeeping gene, β-actin, is expressed in both environments.

Shown in Figure 2 are two-dimensional redox fluorometric microscope photos of second passage goat MSCs isolated, culture-expanded, and examined as detailed in Materials and Methods. Figure 2A and 2D demonstrate low-density and higher-density clustered cells, respectively, excited in the region of 366 nm and emission detected in the region of 450 nm (channel 1). Figure 2B and 2E show the same cells excited around 460 nm and detected around 540 nm (channel 2). Figure 2C and 2F are unprocessed overlaid images of the previous image sets, with the 450 nm emission (channel 1) pseudocolored green and the 540 nm emission (channel 2) pseudocolored red.

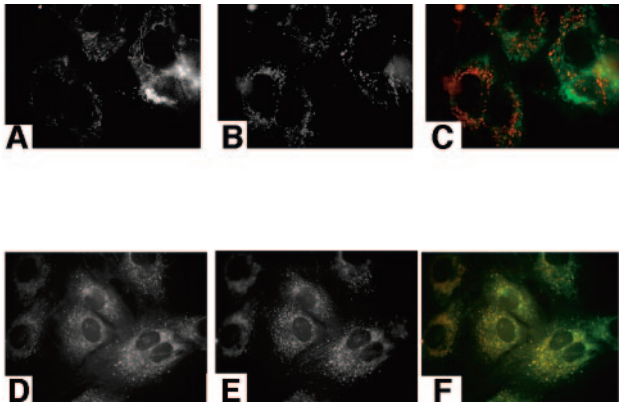

Figure 2. Two-dimensional redox fluorometric microscope photos comparing low-density and higher-density goat mesenchymal stem cell (MSC) cultures. **(A–C):** Low-density (500 cells/cm^2) MSCs. **(A):** Channel 1 (green). **(B):** Channel 2 (red). **(C):** Overlay image. **(D–F):** Higher-density (1,000 cells/cm^2) clustered MSCs **(D):** Channel 1 (green). **(E):** Channel 2 (red). **(F):** Overlay image.

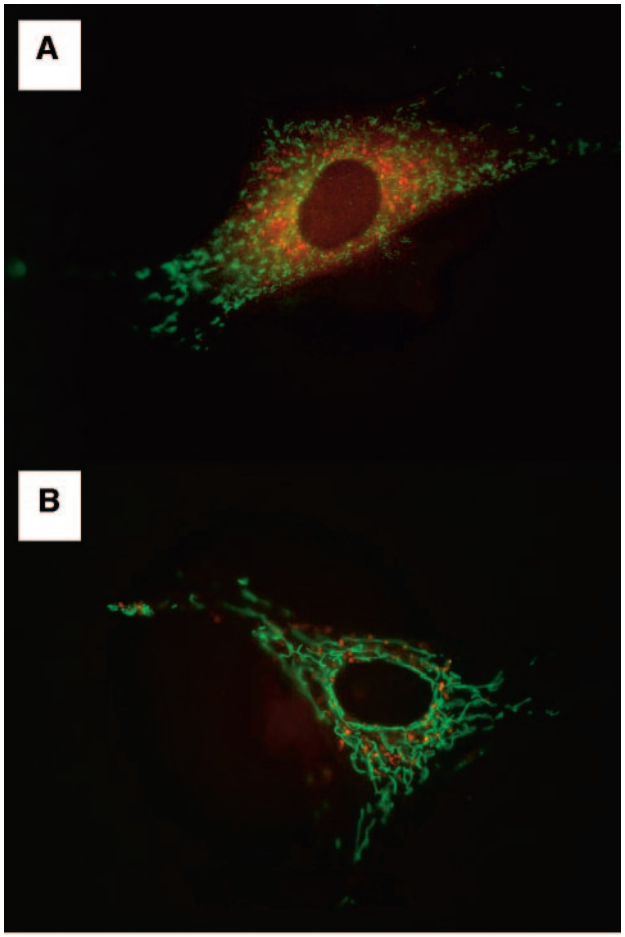

Figure 3. Labeled mitochondria (green) and lysosomes (red) in single mesenchymal stem cells in stem cell growth medium **(A)** and osteogenic medium **(B)**.

Figure 3 demonstrates costaining with MitoTracker and LysoTracker dyes in single cells. Figure 4 demonstrates low-density single cell (Fig. 4A–4C) and higher-density clustered

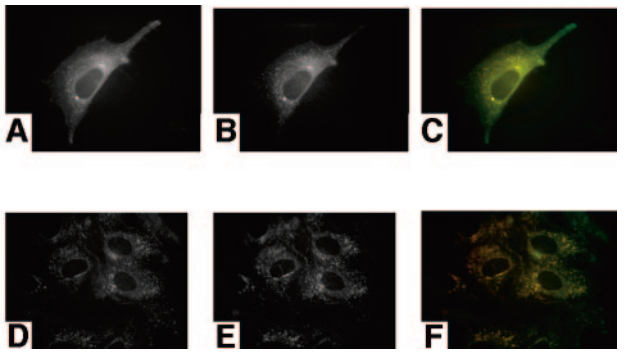

Figure 4. Two-dimensional redox fluorometric microscope photos comparing low-density single cell and higher-density clustered mesenchymal stem cell (MSC) cultures differentiated in osteogenic medium. **(A–C):** Low-density (500 cells/cm^2) MSCs differentiated in osteogenic medium. **(A):** Channel 1 (green). **(B):** Channel 2 (red). **(C):** Overlay image. **(D–F):** Higher-density (1,000 cells/cm^2) clustered MSCs. **(D):** Channel 1 (green). **(E):** Channel 2 (red). **(F):** Overlay image.

(Fig. 4D–4F) MSC cultures differentiated in osteogenic medium for 1 week fluorescing in channel 1 (Fig. 4A, 4D) and channel 2 (Fig. 4B, 4E). As shown, the cytoarchitectural detail of the observed autofluorescence appears to change noticeably, with more apparent overlap (yellow in the overlaid pseudocolor images in Fig. 4C, 4F) of the detected pyridines and flavoproteins. This change from the stem cell to the further differentiated state was confirmed by calculating the ratio of the isolated cell fluorescence intensities (channel 1/channel 2) after subtracting the backgrounds in a series of samples (Table 1).

DISCUSSION

We have demonstrated that redox fluorometry imaging of MSCs expanded in culture is feasible. Moreover, besides providing simple metabolic information, reasonably detailed cytoarchitecture is also visible. Originally, we had expected that nearly all of the stimulated autofluorescence observed would arise from superimposed mitochondrial compartments. However, as displayed in the overlaid images in Figure 2C and 2F, there is separation of the two pseudocolored compartments (green and red), especially in the nonclustered cell image in Figure 2C, with less blended (yellow) overlap than expected. The reduced pyridine species, stimulated at 366 nm, appear to fluoresce in a mitochondrial pattern (green), whereas the oxidized flavoproteins, stimulated at 460 nm, appear to be compartmentalized into a combination of mitochondria and lysosomes/peroxisomes (red). This was not completely unexpected, though, as a significant fraction of flavin-associated autofluorescence is non-redox-responsive, although most of this fluorescence is quenched when bound as protein cofactors. The remaining observed non-redox-responsive fluorescence has been found to not colocalize with mitochondrial subcellular markers but rather with lysosomal markers [9]. To confirm these subcellular anatomic locations, secondary staining with MitoTracker and LysoTracker dyes (Molecular Probes) was performed (Fig. 3).

As expected, the pyridine/flavoprotein ratio decreases upon transitioning from the stem cell to the differentiated state, indicative of an altered metabolic state. That is, decreased cellular respiration is expected to result in an increase in the reduced pyridine nucleotide fluorescence signal (channel 1) and in a decrease in the oxidized flavoprotein fluorescence signal (channel 2), that is, overall increase in the channel 1/channel 2 ratio. Upon an increase in the cellular metabolic machinery, this ratio is expected to decrease, as we observed. Also of note, though, is that significant differences are noted between low-density and high-density clustered cell cultures.

Commitment of stem cells to separate lineages appears to be regulated by multiple cues in the local tissue environment, including mechanical ones that appear to be integral to the commitment of their fate [23]. Altering the redox state of embryonic cells through enzymes has been shown to affect transcription factors and modify gene expression patterns to influence totipotentiality and ultimate cell lineage [24]. Metabolism, including the parameter of redox potential, in cultured cells is also known to depend on cell density, especially mechanical cell-cell contact, and thus cell density must be considered in maintenance of cell cultures. Work comparing immortalized to nonimmortalized fibroblasts demonstrated that as soon as either type of cell came into contact with one another, the total redox potential dropped [25]. To compare metabolic parameters among different cell types, one should take into account the density-dependence of these factors, especially low-density, single cell versus higher-density and more confluent. Thus, there is a distinct possibility that stem cells may not possess an entirely consistent redox fluorometric signature under different culture conditions and densities. If so, as metabolic rates and subcellular organization may change under varying conditions, we may need to perform a larger number of examinations under different conditions (e.g. medium, substrates, and densities) to more easily separate stem cells from nonstem cells.

MSC cultures are also known to sometimes exist as heterogeneous mixtures of cells with varying potentials, including multi-, bi-, and unipotent progenitors, as well as committed osteoblasts and fibroblasts. Thus, we may be dealing with a heterogeneous mixture of cells with varying potentials, although, as described above, these cells are homogeneously

Table 1. Autofluorescence ratios

Cell type	Pyridine (channel 1)/ flavoprotein (channel 2)	*p* value
1. Low-density MSCs in stem cell medium ($n = 15$)	2.19 ± 0.59	
2. High-density clustered MSCs in stem cell medium ($n = 15$)	1.45 ± 0.27	$p = .0001$ vs. 1
3. Low-density MSCs in osteogenic medium ($n = 15$)	1.38 ± 0.57	$p = .0007$ vs. 1
4. High-density clustered MSCs in osteogenic medium ($n = 15$)	0.87 ± 0.34	$p = .00002$ vs. 2; $p = .007$ vs. 3

Abbreviation: MSC, mesenchymal stem cell.

$SH4^+/CD14^-$ and $CD44^+/CD34^-$. If so, because the redox values reported are random samples of reasonably large numbers of cells from multiple sample plates, they would be representative of average populations under each growth condition. Future studies will address these issues further by using subcloned populations.

Finally, another technical problem that we will need to consider using this one-photon imaging technique is the problem of fluorescence photobleaching of intrinsic fluorophores. However, as described here and throughout the literature, reliable signals may be obtained if the experimental technique is optimized, especially maintenance of low ambient light conditions and decreased exposure times.

Currently there exists no reliable, noninvasive technique to screen for stem cells while in continuous culture. Development of such a technique would not only represent a unique stem cell detection device, but would also provide a viable alternative to the currently popular search for immunomarkers. A major advantage is that such observations can be made noninvasively with quantitative metabolic and cytoarchitectural detail intermittently in live culture.

ACKNOWLEDGMENTS

This work was supported by National Institutes of Health grant EY412-5, Research to Prevent Blindness, and the Stark-Mosher Center for Cataract and Corneal Diseases.

DISCLOSURES

The authors indicate no potential conflicts of interest.

REFERENCES

1 Jaiswal RK, Jaiswal N, Bruder SP et al. Adult human mesenchymal stem cell differentiation to the osteogenic or adipogenic lineage is regulated by mitogen-activated protein kinase. J Biol Chem 2000;275:9645–9652.

2 Ryden M, Dicker A, Gotherstrom C et al. Functional characterization of human mesenchymal stem cell-derived adipocytes. Biochem Biophys Res Commun 2003;311:391–397.

3 Solchaga LA, Welter JF, Lennon DP et al. Generation of pluripotent stem cells and their differentiation to the chondrocytic phenotype. Methods Mol Med 2004;100:53–68.

4 Meinel L, Karageorgiou V, Fajardo R et al. Bone tissue engineering using human mesenchymal stem cells: Effects of scaffold material and medium flow. Ann Biomed Eng 2004;32:112–122.

5 Qian L, Saltzman WM. Improving the expansion and neuronal differentiation of mesenchymal stem cells through culture surface modification. Biomaterials 2004;25:1331–1337.

6 Luo Y, Cai J, Ginis I et al. Designing, testing and validating a focused stem cell microarray for characterization of neural stem cells and progenitor cells. STEM CELLS 2003;21:575–587.

7 Bradford GB, Williams B, Rossi R et al. Quiescence, cycling, and turnover in the primitive hematopoietic stem cell compartment. Exp Hematol 1997;25:445–453.

8 Masters BR, Ghosh AK, Wilson J et al. Pyridine nucleotides and phosphorylation potential of rabbit corneal epithelium and endothelium. Invest Ophthalmol Vis Sci 1989;30:861–868.

9 Rocheleau JV, Head WS, Piston DW. Quantitative NAD(P)H/flavoprotein autofluorescence imaging reveals metabolic mechanisms of pancreatic islet pyruvate response. J Biol Chem 2004;279:31780–31787.

10 Tsubota K, Laing RA, Chiba K et al. Noninvasive metabolic analysis of preserved rabbit cornea. Arch Ophthalmol 1988;106:1713–1717.

11 Piston DW, Masters BR, Webb WW. Three-dimensionally resolved NAD(P)H cellular metabolic redox imaging of the in situ cornea with two photon excitation laser scanning microscopy. J Microsc 1995;178:20–27.

12 Yeh AT, Nassif N, Zoumi A et al. Selective corneal imaging using combined second-harmonic generation and two-photon excited fluorescence. Opt Lett 2002;27:2082–2084.

13 Zoumi A, Yeh A, Tromberg BJ. Imaging cells and extracellular matrix in vivo by using second-harmonic generation and two-photon excited fluorescence. Proc Natl Acad Sci U S A 2002;99:11014–11019.

14 Croce AC, Spano A, Locatelli D et al. Dependence of fibroblast autofluorescence properties on normal and transformed conditions. Role of metabolic activity. Photochem Photobiol 1999;69:364–374.

15 Zhang JC, Savage HE, Sacks PG et al. Innate cellular fluorescence reflects alterations in cellular proliferation. Lasers Surg Med 1997;20:319–331.

16 Smith J, Ladi E, Mayer-Proschel M et al. Redox state is a central modulator of the balance between self-renewal and differentiation in a dividing glial precursor cell. Proc Natl Acad Sci U S A 2000;97:10032–10037.

17 Williams CG, Kim TK, Taboas A et al. In vitro chondrogenesis of bone-marrow derived mesenchymal stem cells in a photopolymerizing hydrogel. Tissue Engineering 2003;9:679–688.

18 Jaiswal N, Haynesworth SE, Caplan AI et al. Osteogenic differentiation of purified, culture-expanded human mesenchymal stem cells in vitro. J Cell Biochem 1997;64:295–312.

19 Murphy JM, Fink DJ, Hunziker EB et al. Stem cell therapy in a caprine model of osteoarthritis. Arthritis Rheum 2003;48:3464–3474.

20 Pittenger MF, Mackay AM, Beck SC et al. Multilineage potential of adult human mesenchymal stem cells. Science 1999;284:143–147.

21 Barry FP, Murphy JM. Mesenchymal stem cells: Clinical applications and biological characterization. Int J Biochem Cell Biol 2004;36:568–584.

22 Yang F, Williams CG, Wang D et al. The effect of incorporating RGD adhesive peptide in polyethylene glycol diacrylate hydrogel on osteogenesis of bone marrow stromal cells. Biomaterials 2005;26:5991–5998.

23 McBeath R, Pirone DM, Nelson CM et al. Cell shape, cytoskeletal tension, and RhoA regulate stem cell lineage commitment. Dev Cell 2004;6:483–495.

24 Guo Y, Einhorn L, Kelley M et al. Redox regulation of the embryonic stem cell transcription factor Oct-4 by Thioredoxin. STEM CELLS 2004;22:259–264.

25 Bereiter-Hahn J, Munnich A, Woiteneck P. Dependence of energy metabolism on the density of cells in culture. Cell Struct Funct 1998;23:85–93.